

# Molecular Dynamics Simulation of a Class A $\beta$ -Lactamase: Structural and Mechanistic Implications

S. Vijayakumar, G. Ravishanker, R. F. Pratt,\* and D. L. Beveridge\*

Contribution from the Hall-Atwater Laboratories, Department of Chemistry, Wesleyan University, Middletown, Connecticut 06459

Received July 7, 1994<sup>⊗</sup>

**Abstract:** A molecular dynamics (MD) simulation of the class A  $\beta$ -lactamase from *S. aureus* PC1 has been carried out based on the GROMOS force field. The simulation treats the enzyme solvated by 7295 molecules of water in a hexagonal prism cell using periodic boundary conditions. The overall structural integrity of the molecule is well preserved. Calculated temperature factors show no dramatic increase in the flexibility of the  $\Omega$  loop, a loosely packed 17-residue segment (residues 163–179) adjacent to the active site. The salt bridge between Arg164 and Asp179, believed to be the main stabilizing interaction for the  $\Omega$  loop, was observed to be destabilized in the theoretical model but is compensated in part by a new interaction between Arg164 and Glu168. Early in the simulation, however, a rigid flap-like motion was observed for the  $\Omega$  loop which results in a repositioning of the carboxylate group of Glu166 within hydrogen-bonding distance of the primary nucleophile, the Ser70 hydroxyl group, coupled with displacement of the “hydrolytic” water molecule. The significant repositioning of Glu166 suggests that its position in the crystal structures of class A  $\beta$ -lactamases cannot be taken as conclusive evidence that an acylation mechanism involving direct general base catalysis by the Glu166 carboxylate is incorrect. Analysis of the mobility of active site water molecules suggests that most of them, including the “hydrolytic” and “oxyanion hole” water molecules, exchange with bulk solvent much faster than the catalytic time scale.

## Introduction

The  $\beta$ -lactamases are bacterial enzymes that inactivate  $\beta$ -lactam antibiotics by catalyzing the hydrolysis of the amide group of the  $\beta$ -lactam ring.<sup>1</sup> They are thus the source of much bacterial resistance to these antibiotics. In recent years, the therapeutic effectiveness of many  $\beta$ -lactam antibiotics has been compromised by the emergence of strains of bacteria that are resistant to even new generation  $\beta$ -lactams because they carry  $\beta$ -lactamase mutants of relevant specificity.<sup>2,3</sup> It is therefore important that the structure and function of the  $\beta$ -lactamases be studied in considerable detail. One goal of such studies would, of course, be the design of novel  $\beta$ -lactamase inhibitors and antibiotics.

The most intensively studied  $\beta$ -lactamases are probably those of class A enzymes.<sup>4</sup> Structural studies, in particular, are now well-advanced, and six different crystal structures of class A  $\beta$ -lactamases have been described. The structure of the *Staphylococcus aureus* PC1 enzyme has been determined and refined at 2 Å resolution<sup>5,6</sup> and that of the *Bacillus licheniformis*  $\beta$ -lactamase at 2 Å resolution.<sup>7</sup> Preliminary accounts of the structure of the enzyme from *Streptomyces albus* G at 3 Å<sup>8</sup> and of *Bacillus cereus*  $\beta$ -lactamase I<sup>1</sup> have appeared, and most recently, the results of two independent determinations of the structure of the enzyme of the TEM plasmid have been published.<sup>9,10</sup> In addition, the structure of a penicilloyl-enzyme intermediate of a weakly-active TEM mutant has been de-

scribed,<sup>9</sup> and that of the *S. aureus* enzyme modified by a specific phosphonate inhibitor in order to produce a transition state analogue structure.<sup>11</sup>

The gross structure of these class A  $\beta$ -lactamases are all very similar, reflecting their considerable amino acid sequence homology, and the active site regions are essentially identical. The active site cavity contains, presumably specifically-placed, conserved residues thought to be crucial to catalysis, Ser70 (the consensus sequence numbering of Ambler et al.<sup>12</sup> is used in this paper), the primary nucleophile of the well-established double displacement mechanism, Lys73, Lys234, Ser130, and Glu166. Despite the details of the active site structure available from crystallography, described above, there seems to be no general agreement on how the above-mentioned residues, apart from Ser70, participate in catalysis.<sup>13,14</sup>

A common, unique feature of class A  $\beta$ -lactamases is the  $\Omega$  loop, 17 residues long (residues 163–179) and devoid of any extended secondary structure. It is anchored, seemingly rather loosely, to the body of the main protein and forms one wall (or the floor, in the orientation presented by Moews et al.<sup>7</sup>) of the active site. The final conformation of the loop in the active enzyme appears to require a cis peptide between residues 166 and 167. In the *B. licheniformis* and TEM enzymes, the cis peptide adjoins a proline residue (Pro167), but in the *S. aureus*, more unusually, the cis peptide is formed between Glu166 and Ile167. The conformation and flexibility of the loop is important to  $\beta$ -lactamase catalysis because Glu166 is conserved in class A  $\beta$ -lactamases as an active site residue. As a carboxylate anion, it has been proposed to play the role of a general base in

<sup>⊗</sup> Abstract published in *Advance ACS Abstracts*, January 15, 1995.

(1) Waley, S. G. In *The Chemistry of  $\beta$ -Lactams*; Page, M. I., Ed.; Chapman & Hall: London, 1992; p 198.

(2) Neu, H. C. *Science* **1992**, *257*, 1064.

(3) Moellering, R. C., Jr. *J. Antimicrob. Chemother.* **1993**, *31*, Suppl. A, 1.

(4) Ambler, R. P. *Phil. Trans. R. Soc. London* **1980**, *289*, 321.

(5) Herzberg, O.; Moul, J. *Science* **1987**, *236*, 694.

(6) Herzberg, O. *J. Mol. Biol.* **1991**, *217*, 701.

(7) Moews, P. C.; Knox, J. R.; Dideberg, O.; Charlier, P.; Frere, J.-M. *Proteins: Struct., Funct. Genet.* **1990**, *7*, 156.

(8) Dideberg, O.; Charlier, P.; Wery, J. P.; Dehottay, P.; Dusart, J.; Ericpicum, T.; Frere, J.-M.; Ghuysen, J.-M. *Biochem. J.* **1987**, *245*, 911.

(9) Strynadka, N. C. J.; Adachi, H.; Jensen, S. E.; Johns, K.; Sielecki, A.; Betzel, C.; Sutoh, K.; James, M. N. G. *Nature* **1992**, *359*, 700.

(10) Jelsch, C.; Mourey, L.; Masson, J.-M.; Samama, J.-P. *Proteins: Struct., Funct. Genet.* **1993**, *16*, 364.

(11) Chen, C. C. H.; Rahil, J.; Pratt, R. F.; Herzberg, O. *J. Mol. Biol.* **1993**, *234*, 165.

(12) Ambler, R. P.; Coulson, A. F. W.; Forsman, M.; Tiraby, G.; Frere, J.-M.; Ghuysen, J. M.; Joris, B.; Levesque, R. C.; Waley, S. G. *Biochem. J.* **1991**, *276*, 269.

(13) Fink, A. L. *Chemtracts-Biochem. Mol. Biol.* **1992**, *3*, 395.

(14) Rahil, J.; Pratt, R. F. *Biochemistry* **1994**, *33*, 116.

catalysis,<sup>1,15,16</sup> analogously to His57 in chymotrypsin, although, more recently, some have suggested that it plays this role only during the deacylation step, as a catalyst of the attack on the acyl-enzyme by an occluded water molecule.<sup>9,17-20</sup>

Although analyses of the thermal factors of the loop residues in the available crystal structures do not suggest that the  $\Omega$  loop is significantly more mobile than the bulk of the enzyme,<sup>6,10,21</sup> there has been suspicion that it may have greater mobility in solution. Indeed, it has been suggested that motion of the loop may be involved in the induced fit of substrates into the active site and in the conformational change thought to be the cause of the transformation of the acyl-enzymes formed with penicillins of bulky side chains into inert forms.<sup>5-7,22</sup> The very weakly active P54 mutant of the *S. aureus*  $\beta$ -lactamase, where the single site mutation is of a residue at the end of the loop (D179N<sup>4</sup>), and which in solution has the properties of a late folding intermediate,<sup>23</sup> is observed in the solid state to have a disordered  $\Omega$  loop and a consequently disrupted active site.<sup>24</sup> In the TEM  $\beta$ -lactamase the  $\Omega$  loop appears more constrained by internal salt bridges than in the *S. aureus* PC1 and *B. licheniformis* enzymes<sup>10</sup>; the TEM enzyme seems also less susceptible to substrate-induced inactivation.<sup>25</sup>

We describe in this paper a theoretical model for the class A  $\beta$ -lactamase from *S. aureus* PC1 in dilute aqueous solution developed from a molecular dynamics (MD) simulation. On the basis of a 180-ps dynamical trajectory, the overall structural stability of the protein is examined, along with the dynamics of specific active site residues and water molecules related to  $\beta$ -lactamase catalysis, and the  $\Omega$  loop. The latter results are discussed in terms of current thinking on the mechanism of  $\beta$ -lactamase catalysis. MD provides a new window into enzymic mechanisms, where, using as a starting point the best available structural information, the crystal structure of the enzyme, the likely conformations of the enzyme active site in solution can be explored and related to possible chemical mechanisms. Other examples of this approach to enzymology include studies of the *Streptomyces* R61 DD-peptidase,<sup>26</sup> acylchymotrypsins,<sup>27,28</sup> and HIV-1 protease.<sup>29</sup> The present work provides a base of information from which  $\beta$ -lactamase inhibitor complexes will be examined.

## Methods

The point of departure for this study was the X-ray crystal structure of  $\beta$ -lactamase from *S. aureus* PC1, solved by Herzberg,<sup>9</sup> and included the 16 water molecules (out of 207) identified as structural waters.

(15) Gibson, R. M.; Christensen, H.; Waley, S. G. *Biochem. J.* **1990**, *272*, 613.

(16) Knap, A.; Pratt, R. F. *Biochem. J.* **1991**, *273*, 85.

(17) Herzberg, O.; Moul, J. *Curr. Opin. Struct. Biol.* **1991**, *1*, 946.

(18) Escobar, W. A.; Tan, A. K.; Fink, A. L. *Biochemistry* **1991**, *30*, 10783.

(19) Adachi, H.; Ohta, T.; Matzuzawa, H. *J. Biol. Chem.* **1991**, *266*, 3186.

(20) Knox, J. R.; Moews, P. C.; Escobar, W. A.; Fink, A. L. *Protein Eng.* **1993**, *6*, 11.

(21) Knox, J. R.; Moews, P. C. *J. Mol. Biol.* **1991**, *220*, 435.

(22) Pratt, R. F. In *The Chemistry of  $\beta$ -Lactams*; Page, M. I., Ed.; Chapman & Hall: London, 1992; p 229.

(23) Craig, S.; Hollecker, N.; Creighton, T. E.; Pain, R. H. *J. Mol. Biol.* **1985**, *185*, 681.

(24) Herzberg, O.; Kapadia, G.; Blanco, B.; Smith, T. S.; Coulson, A. *Biochemistry* **1991**, *30*, 9503.

(25) Citri, N.; Kalkstein, A.; Samuni, A.; Zyk, N. *Eur. J. Biochem.* **1984**, *144*, 333.

(26) Boyd, D. B.; Snoddy, J. D.; Lin, H.-S. *J. Comput. Chem.* **1991**, *12*, 635.

(27) Bemis, G. W.; Carlson-Golab, G.; Katzenellenbogen, J. A. *J. Am. Chem. Soc.* **1992**, *114*, 570.

(28) Nakagawa, S.; Yu, H.-A.; Karplus, M.; Umeyama, H. *Proteins: Struct., Funct. Genet.* **1993**, *16*, 172.

(29) Harte, W. E.; Beveridge, D. L. *J. Am. Chem. Soc.* **1993**, *115*, 3883.

The protein was solvated with an additional 7279 molecules of water in a hexagonal prism of height 71.3 Å and an inscribed circular radius of 34.6 Å, so that the resultant density was 1 g/cm<sup>3</sup>. The protonation states for charged residues were decided based on their ionization states at pH 7.0. Thus, charges for Glu and Asp were set to -1e and those for Lys and Arg to +1e. The side chains of the two histidines were neutral. The system was treated in the simulation under periodic boundary conditions. The simulation protocol included an initial solvent relaxation of 131M configurations of Metropolis Monte Carlo simulation, followed by 750 steps of conjugate gradient minimization of the entire system. This was followed by a heating step, wherein the temperature of the entire system was raised to 300 K over 1.5 ps, a Gaussian equilibration step for 3.5 ps, an unconstrained MD equilibration for 25.0 ps, and a trajectory for a duration of 150.0 ps. The temperature window was 5 K during the equilibration stages and 10 K during the trajectory.

Molecular dynamics calculations in this study were performed with the Monte Carlo (MC) and MD simulation program WESDYN.<sup>30</sup> The RT37C4 force field of GROMOS86<sup>31</sup> and the SPC model<sup>32</sup> for water were used for the solution studies. The GROMOS force field employs a united hydrogen atom on nonpolar groups and an explicit hydrogen atom on polar groups. Switching functions were used to make the long-range nonbonded interactions go smoothly to zero between 7.5 Å and 8.5 Å, and applied on a group-by-group basis to avoid artificially splitting dipoles. The above cutoff has been employed to minimize the computational cost and accomplish large scale simulation of this magnitude. With this approach, the protein is well-behaved; however, highly charged systems may be susceptible to inaccuracies. The calculations were carried out on the CRAY YMP/8-32 at the Pittsburgh Supercomputer Center, and required ca. 260 h of machine time.

Solvent analysis for the active site residues was carried out by analyzing the first hydration shell, based on a distance criterion (distances were calculated based on heavy atom positions), which included waters within 3.5 Å of the side chain functional groups. The most probable water hydrating a given side chain functional group was then determined, and the trajectory of these water molecules was analyzed. Conformational analysis was carried out using the "Dials and Windows" utility in the MD Toolchest,<sup>33</sup> which produces time evolution of the variation of all dihedral angles in the protein. Root-mean-square (RMS) deviations were calculated by individually superposing the selected atoms, rather than the entire protein, in order to discount translation and rotational effects between subdomains.

## Results

The convergence indices for the simulation, namely, total energy, temperature, and RMS deviation with respect to the crystal form, are shown in Figure 1. The total energy of the system (1A) and temperature (1 B) goes through a series of rescalings during equilibration and remains conserved during the entire production phase of the simulation. The time evolution of RMS deviation (1 C) of the MD trajectory is shown for all atoms (solid line) and backbone atoms of the entire protein (dashed line). The all atom deviation levels off at about 2.5 Å. However, the maximum RMS deviation of the backbone atoms is only about 1.8 Å. The relatively small value for the all atom and backbone RMS deviations coupled with a conserved total energy suggests the simulation to be stable and sufficiently close to the crystal form.

The overall motion and dynamical structure of the protein is presented in Figure 2a. The  $\alpha$  carbon traces from six snapshots obtained from the MD trajectory at 30-ps intervals are super-

(30) Ravishanker, G.; Swaminathan, S.; Beveridge, D. L. *WESDYN 2.0*; Wesleyan University: Middletown, CT 06459.

(31) van Gunsteren, W. F.; Berendsen, H. J. C. *GROMOS86*; University of Groningen: Groningen.

(32) Berendsen, H. J. C.; Postma, J. P. M.; van Gunsteren, W. F.; Hermans, J. *Interaction Models for Water in Relation to Protein Hydration*; D. Reidel: Dordrecht, 1981.

(33) Ravishanker, G.; Beveridge, D. L. *MD Toolchest*; Wesleyan University: Middletown, CT 06459.

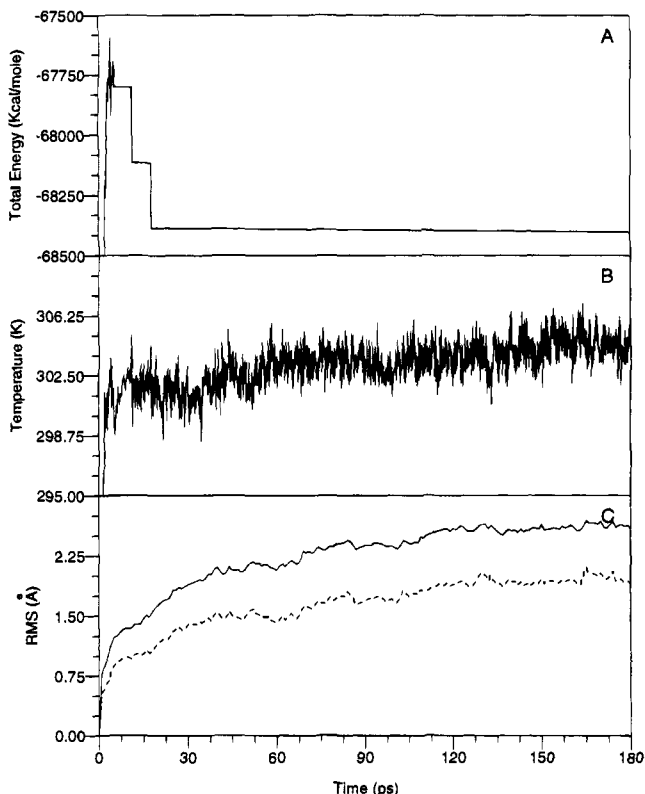


**Figure 1.** Convergence criteria for the simulation. Time evolution of the total energy (A), temperature (B), and RMS deviation of the MD trajectory with respect to the crystal form (C).

posed over that from the crystal structure. It is apparent that the secondary structural regions are fairly rigid, and significant deviations from the crystal structure are seen only in the loops and turns. Exactly where do the RMS deviations arise? Figure 2b shows the breakdown of the RMS deviations between secondary structures (helices and sheets, SS),  $\Omega$  loop (OL), and other loops and turns (L&T). The segregation of the RMS deviations into distinct structural types provides some insight into the origin of these effects, supporting the observation that the bulk of the deviations arise from the loops in the protein while the secondary structure is relatively intact. Interestingly, the  $\Omega$  loop undergoes a distinct conformational transition during a 30-ps period from 70 to 100 ps. Although the magnitude of the RMS deviation is small, it suggests that the  $\Omega$  loop can access alternative conformational states. The conformational change involved in this transition is graphically depicted and color coded in Figure 3a, which represents average conformations of the  $\Omega$  loop over 30-ps intervals prior to (green), during (blue), and following the transition (red), superposed on the crystal structure (black). A translational motion of the N-terminal section of the  $\Omega$  loop with respect to the crystal structure is obvious, which is toward the active site in the framework of the whole protein. Detailed animation of the dynamics suggests that the initial motion of the  $\Omega$  loop (Figure 3a, black vs green line) is similar to that of a rigid flap where the N-terminal portion (residues 164–173) moves much closer to the active site and the C-terminal portion (residues 174–179) moves outward. Significant conformational changes were subsequently observed (Figure 3a, blue and red lines) in the C-terminal section of the loop (Figure 3b) involving further movement outward, while the N-terminal half containing the catalytic residue, Glu166, remained relatively rigid and close to the active site. More detailed conformational analysis has been carried out using “Dials and Windows” and is discussed below. We have further examined concerted motions between

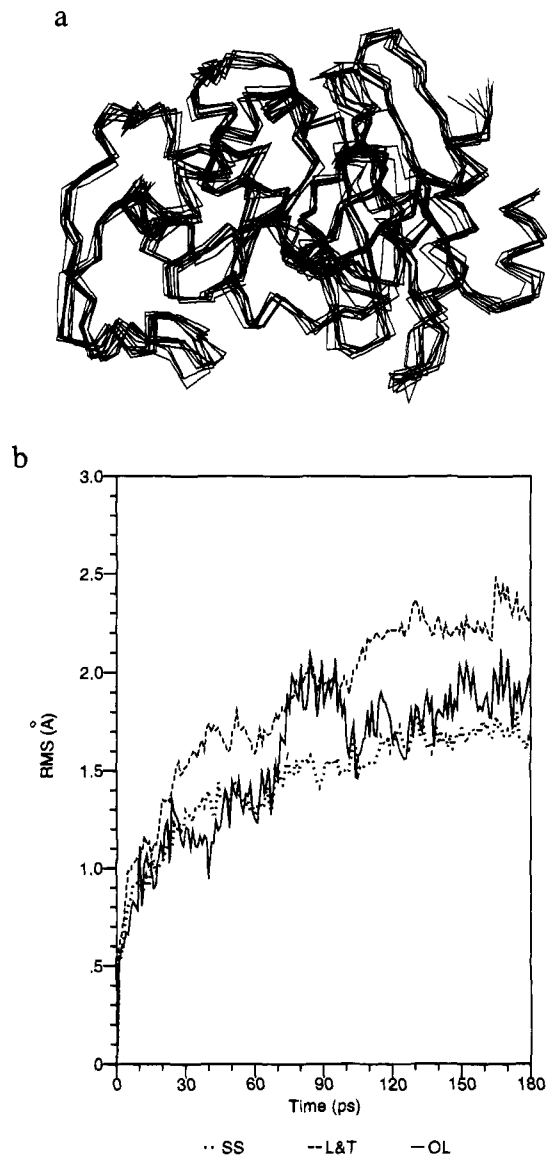


**Figure 2.** (a)  $\alpha$ -Carbon drawings of six structures obtained from the MD trajectory, at equally spaced intervals (30 ps), overlaid on top of the crystal structure, to illustrate the nature of the structural deviations and the proximity of the trajectory to the crystal form. (b) Breakdown of the RMS deviations between secondary structures, helices and sheets, (SS),  $\Omega$  loop (OL), and other loops and turns (L&T).

the active site residues and the conformational changes in the  $\Omega$  loop, by analyzing the relative disposition of key active site residues. The hydration of the active site is described in the Discussion.

The conformational transition in the  $\Omega$  loop is shown in greater detail in Figure 3b using the procedure of “Dials and Windows”. The  $(\phi, \psi)$  values for residues in the  $\Omega$  loop are presented for the entire trajectory, as a scatter rather than a time evolution, to indicate the range of conformational states accessible to each residue. The 12 o’clock position in each of these dials represents  $0^\circ$  or  $360^\circ$  and the angles increase clockwise. The shadings on the circumference of these dials are normalized probability distributions and indicate the conformational propensities of the backbone dihedral angles of a given residue. It is clear from the above data that residues in the C-terminal portion are accessing a larger number of conformational states compared to those in the N-terminal portion of the  $\Omega$  loop. Specifically, residues 175–179 have a larger spread in  $(\phi, \psi)$  angles. Although it is impossible to infer anything specific from

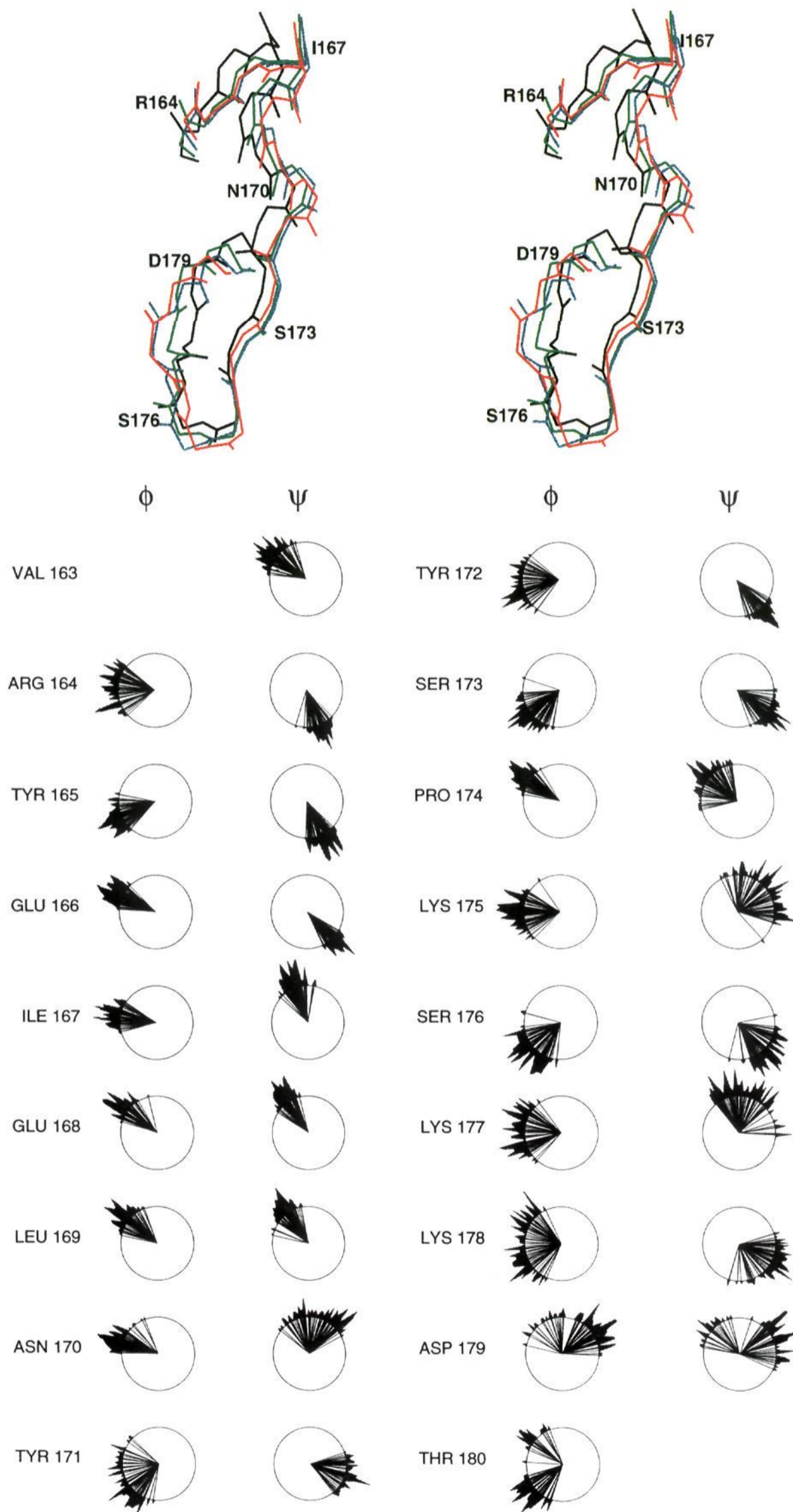


**Figure 3.** (a, top) Average conformations (over 30 ps) of the  $\Omega$  loop obtained prior to (green), during (blue), and following the transition (red) illustrated in Figure 2b, superposed on the crystal structure (black). (b, bottom) Analysis of the dynamical changes in the backbone dihedral angles ( $\phi$ ,  $\psi$ ) of the residues located in the  $\Omega$  loop. The 12 o'clock position in each of these dials represents 0° or 360° and the angles increase clockwise. The shading on the circumference of these dials represents the normalized probability distribution and indicates the conformational propensities of the backbone dihedral angles of a given residue.

the conformational preferences of individual residues, the collective effect of these individual propensities can lead to a

large number of conformational possibilities for the overall loop (see Figure 3a for a graphical presentation). Subtle conforma-

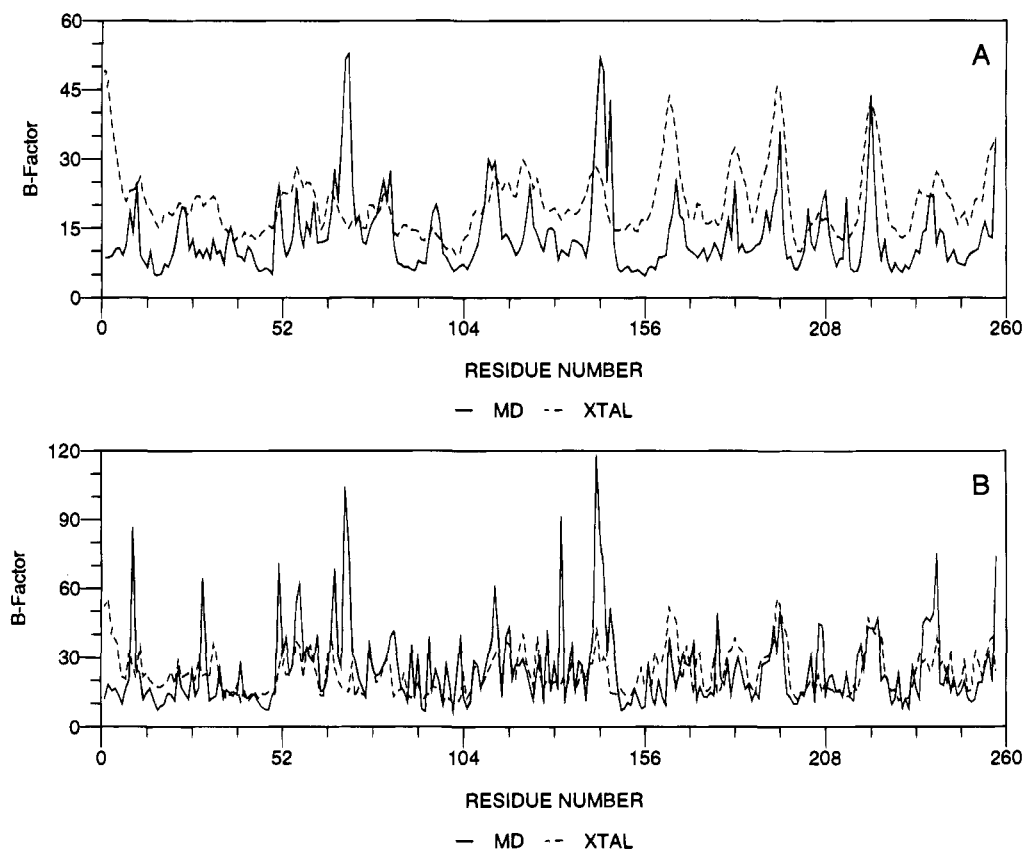


**Figure 4.** Comparison of MD derived B-factors ( $\text{\AA}^2$ ) with X-ray diffraction data. Panel A corresponds to backbone atoms and panel B to side chain atoms.

tional changes such as this might appear to be unimportant structurally, but they may bear upon the activity of the enzyme.

The overall features of the MD derived B-factors (solid line) are in qualitative agreement with the experiment (X-ray diffraction data, dashed line) (Figure 4). Two distinct regions are obvious for the  $\Omega$  loop, the MD derived B-factors for the N-terminal portion being substantially lower than that of the C-terminal section. The value for the C-terminal portion is higher compared to the secondary structural regions but comparable to other loop regions of the protein, distinguished by peaks at around residues 100, 225, and 250. The lower value of the calculated thermal factors with respect to X-ray diffraction data can be attributed to the removal of translation and rotation from the calculations and the short duration of the MD trajectory.

Figure 5a is a plot of the time evolution of the distance ( $\text{\AA}$ ) between residues located on the  $\Omega$  loop and those related to the catalytic mechanism and stabilization of the  $\Omega$  loop, via electrostatic and hydrogen bond interactions (see Figure 6a for a view of the active site in the crystal conformation). Reported here are the distances for the interaction between Asn170 [O $\delta$ ] and the carboxylate oxygens of Glu166 [solid line, O $\epsilon$ 1; dashed line, O $\epsilon$ 2] and for the salt bridges, Lys73 [N $\zeta$ ]-Glu166 [solid line, O $\epsilon$ 1; dashed line, O $\epsilon$ 2] and Arg164 [N $\delta$ 2]-Asp179 [O $\delta$ 1]. The proximity of both the carboxylate oxygens of Glu166 with respect to Asn170 [N $\delta$ ] (data not shown) is similar to that found in the crystal structure; however, one of the carboxylate oxygens, Glu166 [O $\epsilon$ 2], is closer to the Asn170 [O $\delta$ ] by about 1  $\text{\AA}$  on the average. Such arrangements can be achieved through rotation of the side chain functional groups of Asn170 and Glu166, which can further help to orient and activate the "hydrolytic" water (see Discussion). As for salt bridges, both appear to weaken during the simulation, that of Arg164-Asp170 considerably more than Glu166-Lys73. Crystallographic and MD average distance between Glu166 and Lys73 are 2.8 (for

O $\epsilon$ 1) and 3.4  $\text{\AA}$  (for O $\epsilon$ 2), respectively. The former salt bridge between Arg164-Asp179, at the base of the  $\Omega$  loop, is suspected to stabilize the loop conformation.<sup>6</sup> During this simulation it was found to vary from about 2.8  $\text{\AA}$  in the crystal structure to about 7.4  $\text{\AA}$  with an average distance of 5.0  $\text{\AA}$ . The loss of this electrostatic interaction is compensated in part by the formation of a new interaction between Arg164 and Glu168 (data not shown), the distance between them found to be at an average of 6.1  $\text{\AA}$  and being only 3.1  $\text{\AA}$  at the closest approach. The destabilization of the salt bridge between Arg164 and Asp179 has been attributed to be cause of the dramatic increase in flexibility in the mutant enzyme P54.<sup>24</sup> The structure of the mutant and that of the native enzyme are very similar (RMSD of C $\alpha$  atoms is  $\sim$ 0.45  $\text{\AA}$ ), and, yet, the destabilization of this salt bridge in our simulation shows only a moderate increase in the calculated thermal factors and not as dramatic as in the mutant enzyme (compare Figure 5 and Figure 2 in Herzberg et al.<sup>24</sup>). More detailed comparisons are necessary for a complete understanding of the origin of these effects.

Dynamical fluctuations in the active site residues (Figure 5b) indicate that the range of motion is largest for two key residues, Lys73 and Glu166. The distances ( $\text{\AA}$ ) between various residues are measured with respect to the following atoms: N $\zeta$  for Lys73 and Lys234, O $\gamma$  for Ser70 and Ser130, backbone amide nitrogen, N, for Gln237, and the carboxylate oxygens, O $\epsilon$ 1 and O $\epsilon$ 2, for Glu166. The second panel for distance between Glu166 and Ser70 corresponds to the carboxylate oxygen O $\epsilon$ 1 of Glu166 and the third panel that of O $\epsilon$ 2. Glu166, which is at least 4.0  $\text{\AA}$  away from Ser70 in the crystal structure, was found at an average distance of 2.8  $\text{\AA}$ , and 2.5  $\text{\AA}$  at the closest. Lys73, on the other hand, moved as far away as 6.4  $\text{\AA}$  from Ser70 and averaged at 4.3  $\text{\AA}$ , the corresponding distance in the crystal structure being 2.54  $\text{\AA}$ . The proximity of Ser130 to Ser70 is slightly longer than in the crystal structure, the average and

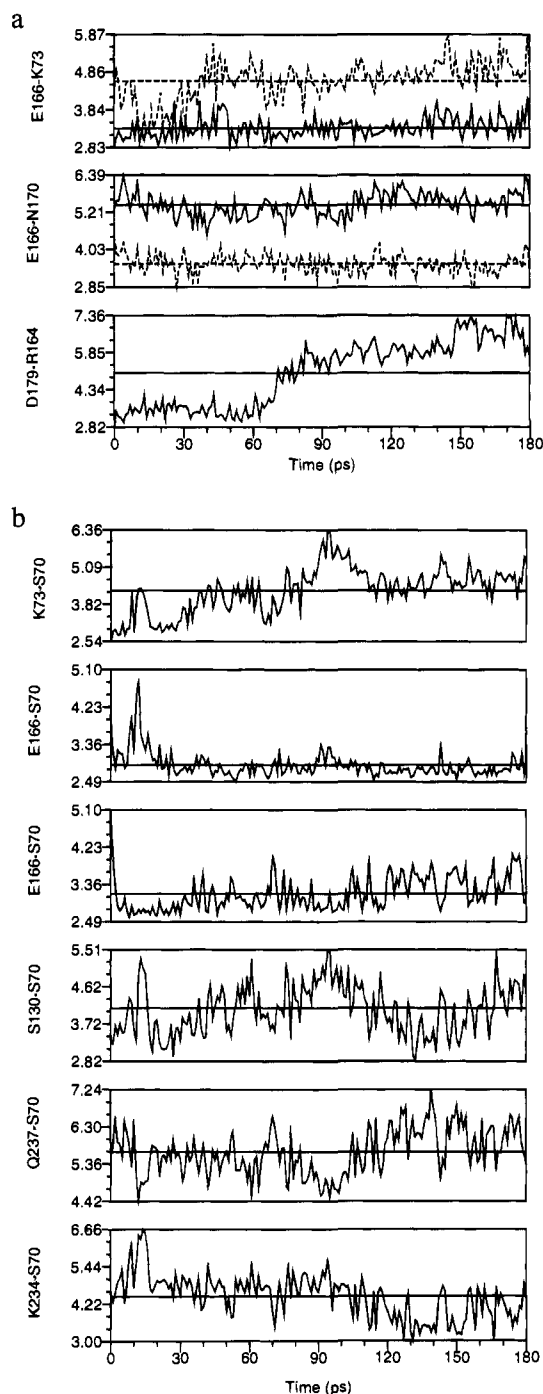


**Figure 5.** (a) Time evolution of the distance (Å) between residues located on the  $\Omega$  loop and those related to the catalytic mechanism and stabilization of the  $\Omega$  loop. The horizontal line through each graph represents the average distance calculated over the length of the simulation. The solid and dashed line in the plots for E166 correspond to distances from the two carboxylate oxygens, O $\epsilon$ 1 and O $\epsilon$ 2, respectively. Refer to the text for details of the atoms used in the distance calculation. (b) Dynamical fluctuations in the distances between some of the key residues in the active site. The horizontal line through each graph represents the average distance calculated over the length of the simulation. The second and third panel labeled "E166-S70" correspond to the distance from the two carboxylate oxygens O $\epsilon$ 1 and O $\epsilon$ 2 of Glu166. Refer to the text for details of the atoms used in the distance calculation.

crystallographic distance being 4.1 and 3.3 Å, respectively. Lys234 and Gln237 were found to remain essentially at their crystallographic positions, their average distance from Ser70 varying by no more than 0.1–0.2 Å.

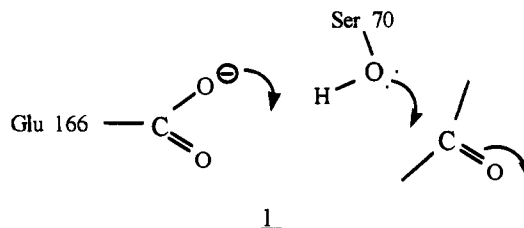
## Discussion

The major issues relating to class A  $\beta$ -lactamase function addressed in this paper are, first, the mobility of the  $\Omega$  loop in solution and its correlation, if any, with the motion of active site residues; second, the dynamic behavior of the critical active site residues themselves; and, third, the time-dependent behavior of water molecules in the active site.

The MD simulation of the *S. aureus* PC1  $\beta$ -lactamase in solution shows that the  $\Omega$  loop is indeed mobile over the 180-ps time interval surveyed, but not as a single unit. The C-terminal region undergoes significant conformational changes, including the transition at around 70 ps concerted with weakening of the salt bridge Arg164–Asp179, illustrated in Figures 3a, 3b, and 4 and described in the Results. It seems likely that this motion would be characteristic of the loop in solution, over this time scale. The N-terminal region, after an distinctive translational motion during the early part of the trajectory, remains largely fixed in place against the bulk of the protein (Figures 3a). The initial flap-like movement may be important to the enzyme activity since its effect is to bring the catalytically essential Glu166 carboxylate group further into the active site (see below) to a position that is maintained for the remainder of the trajectory. It is possible that this "inside" and perhaps reactive conformation of Glu166 is less stable in the weakly active P54 mutant where the  $\Omega$  loop as a whole is likely to be more mobile.<sup>24</sup>

Two of the critical active site functional groups (Figure 5b) undergo striking changes in position during the trajectory. The Glu166 carboxylate, as mentioned above, moves into a position where both oxygen atoms are within hydrogen-bonding distance of the Ser70 hydroxyl group and remains there (particularly O2) throughout the simulation time span. Conversely, the ammonium ion of Lys73, within hydrogen-bonding distance (2.54 Å) of the Ser70 hydroxyl group in the crystal structure, moved away, both from Ser70 and from Glu166, the latter movement being much smaller (0.6 Å). Other active site entities underwent apparently less dramatic motions. The hydroxyl group of Ser130 fluctuated (ca.  $\pm 1$  Å) about a mean slightly further from the Ser70 hydroxyl than in the crystal structure and largely beyond direct hydrogen-bonding distance. The Lys234 ammonium ion fluctuated (also ca.  $\pm 1$  Å), close to the crystallographic distance from Ser70, as did the backbone nitrogen atom of Gln237 which constitutes one component of the oxyanion hole, an important element of catalysis.<sup>34</sup> There does not seem any strong, direct correlation of these motions, relative to the Ser70 hydroxyl group, with the mobility of the C-terminus of the  $\Omega$  loop.

These observations do relate to the mechanism of catalysis, however, in that proposals involving the Glu166 carboxylate as a general base catalyst of nucleophilic attack on the substrate by the Ser70 hydroxyl group, 1,<sup>15,16</sup> have lost support because of the distance between these two functional groups in crystal structures<sup>17</sup> and because of interpretations of the effects of Glu166 mutations on turnover kinetics.<sup>18,19</sup> The latter experi-



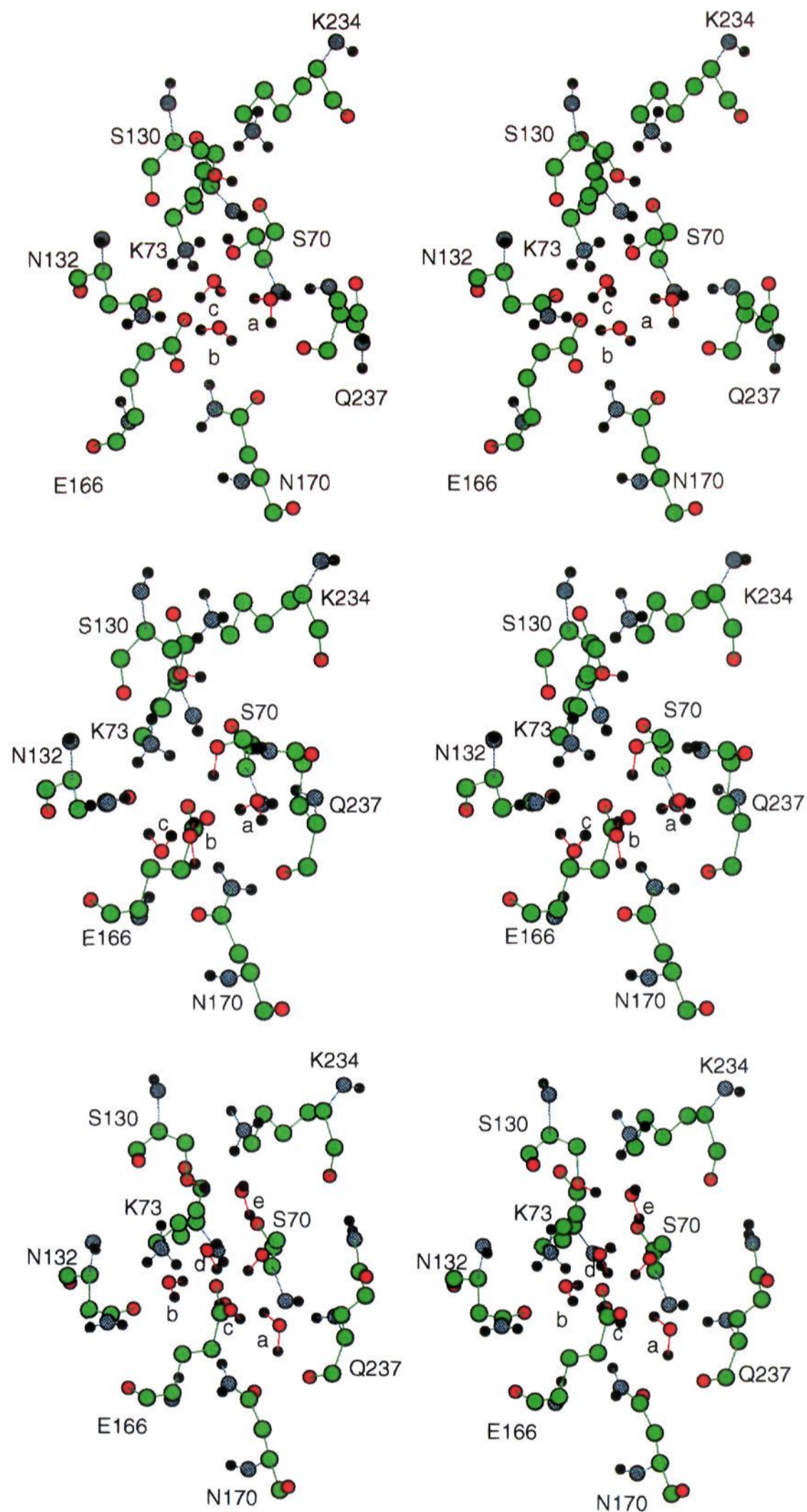


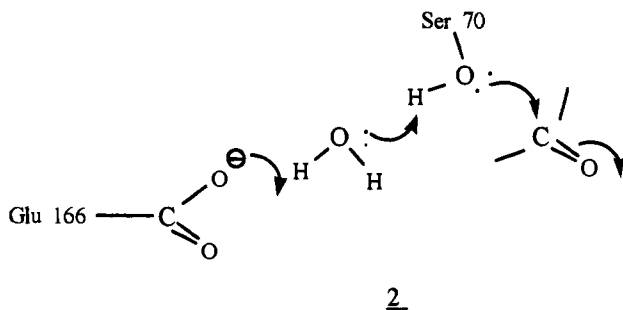
**Figure 6.** (a, top) Arrangement of water molecules in the active site at the end of MC equilibration. Waters **a** and **b** are in the same positions (to within 0.25 Å) as the “oxyanion hole” and “hydrolytic” water molecules of the crystal structures, respectively. Water **c** is a structural water and remains essentially bound to Glu166 [O1]. (b, middle) Snapshot of the active site showing the arrangement of the above water molecules 30 ps into the simulation. (c, bottom) Snapshot of the active site 100 ps into the simulation showing the presence of two additional waters **d** and **e**, which were observed to exchange with the hydrolytic water.

ments are still inconclusive, however, with respect to the acylation step.<sup>1,14</sup> The present results suggest that the inference from the crystal structures should also be regarded as tentative. It seems likely that, in solution, the Glu166 carboxylate can readily achieve direct contact with the active site nucleophile and, in fact, may be stably hydrogen-bonded to it, at least in

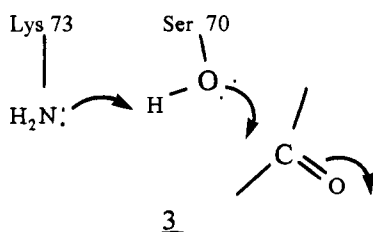
the absence of a substrate. To the extent that one can judge from the structure of the free enzyme, therefore, taking both static and dynamic features into account, **1**, remains a viable mechanism.

The ambiguous position of the Glu166 carboxylate and the presence of the Lys73 ammonium ion directly adjacent to the

Ser70 hydroxyl group in the crystal structures of native class A  $\beta$ -lactamases<sup>5,7,9,10</sup> has given rise to other suggestions for the details of catalysis. In one example, the intervening water molecule between the Glu166 carboxylate and the Ser70 hydroxyl is employed, together with the carboxylate, as an extended general base catalyst in acylation, **2**.<sup>16,35</sup> In another,<sup>9</sup>

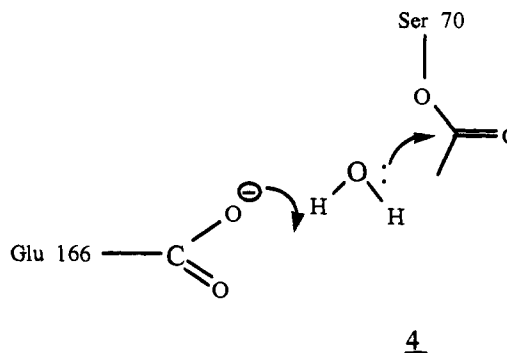


the neutral amine of Lys73 has been proposed to fill the general base role, **3**. The latter suggestion requires that the Lys73



ammonium ion has a rather anomalously low  $pK_a$ , for which there is, at present, no evidence.<sup>13,14,16</sup> The present results obviate the need for the former proposal and do not bear directly on the latter.

The structure of active site water molecules in crystalline class A  $\beta$ -lactamases has been extensively described in the *S. aureus*, *B. licheniformis*, and TEM-1 enzymes.<sup>6,10,21</sup> All three contain two water molecules in the active site which have been implicated in catalysis. One of these water molecules is located at a position close to that identified with the oxyanion hole (the "oxyanion hole" water molecule), within hydrogen-bonding distance of the backbone nitrogen atom of Gln237, somewhat further from the backbone nitrogen of Ser70, and within hydrogen-bonding distance of the Ser70 hydroxyl group. A similarly placed water molecule is found in the oxyanion hole of several serine proteinase crystal structures.<sup>17</sup> Presumably the electrostatic potential of the oxyanion hole focuses a water molecule into this position. A second active site water molecule in the crystal structures has been much discussed. This is found closely associated with the carboxylate group of Glu166(O2), the hydroxyl group of Ser70, and the amide group of Asn170. It has been suggested<sup>6,21</sup> that this water molecule is the one involved in hydrolysis (the "hydrolytic" water molecule) of the acyl-enzyme intermediate in the normal catalytic cycle, where the Glu166 carboxylate directly catalyzes its attack on the acyl-enzyme (**4**). An occluded water molecule is, in fact, seen hydrogen-bonded to Asn166, in the penicilloyl derivative of the Glu166Asn mutant of the TEM-1  $\beta$ -lactamase.<sup>9</sup> These water molecules were not observed in the crystal structures of the weakly active P54 mutant of the *S. aureus* PC1  $\beta$ -lactamase<sup>24</sup> or (although perhaps only displaced) in the Glu166Ala mutant of the *B. licheniformis* enzyme.<sup>20</sup> Several other water molecules were observed across the face of the active site in these structures, although their configuration is probably influenced,



in some cases at least, by anions which also appear to bind at the active site.<sup>10,21</sup>

The present MD simulation provides further insight into the hydration of the active site. The initial MC equilibration of water molecules around  $\beta$ -lactamase, with the enzyme fixed into the crystal structure conformation, yielded the arrangement of water molecules shown in Figure 6a. Waters **a** and **b** are in the same positions (to within 0.25 Å) as the "oxyanion hole" and "hydrolytic" water molecules of the crystal structures, respectively. Also seen is a structural water **c**, hydrogen-bonded to the carboxylate oxygen (O1) of Glu166. The position of the noncrystallographic water molecules **a** and **b**, obtained from MC equilibration, very similar to that observed in the crystal structure, is a reassuring observation.

A snapshot of the active site showing the arrangement of water molecules at 30 ps is seen in Figure 6b. During the initial stage of the simulation, as Gln166 moves into proximity of Ser70, the hydrolytic water **b** remains hydrogen-bonded to Glu166—O2 but, presumably because of the steric interaction with Ser70 and water **a**, is forced in a direction away from Ser70 and the active site. The new position taken up by Glu166 allows the carboxylate oxygen O2 to hydrogen bond not only to the Ser70 hydroxyl group but also to water **a**; the latter remains in close contact with the backbone NH of Gln237 and the Ser70 hydroxyl group. Water **b** remains in contact with Glu166 and water **a** but not with Ser70.

During the subsequent 165 ps (Figure 6c drawn at some 100 ps, with additional waters), the crystallographic water **c** did not exchange with bulk solvent, and the oxyanion hole water **a** exchanged once (although not with water **b**). Somewhat more mobile were a cluster of water molecules (**d** and **e**) positioned between Ser130 and Ser70 and including the extruded erstwhile hydrolytic water molecule **b**. It is possible that one of the latter molecules becomes occluded by a substrate on binding and becomes the real "hydrolytic" water in deacylation, but, in the free enzyme, it seems that all of the above-mentioned water molecules, except perhaps the crystallographic water **c**, would readily exchange with solvent on a nanosecond time scale. The oxyanion hole water **a** would be displaced from its position in Figure 6a and b, by a substrate (the crystal structure of an acyl-enzyme of the Glu166Ala mutant of the TEM-1  $\beta$ -lactamase shows the carbonyl oxygen in the oxyanion hole<sup>9</sup> as is one phosphonyl oxygen of a transition state analogue complex of the PC1 enzyme<sup>11</sup>), but would still be bound to Glu166, and could be constrained by the substrate in the active site and thus become the "hydrolytic" water.

These results show clearly the value of MD calculations to the process of extrapolation of an enzyme crystal structure into an enzyme mechanism. Contacts between functional groups that are essential elements of a mechanism, but which may seem precluded by the solid state structure, may become accessible when the flexibility of the protein in aqueous solution is taken

(35) Lamotte-Brasseur, J.; Dive, G.; Dideberg, O.; Charlier, P.; Frere, J.-M.; Ghuyssen, J.-M. *Biochem. J.* **1991**, *279*, 213.



into account in a rigorous fashion. It is easy to speculate about protein mobility in solution but, in the absence of limits established by some acceptable experimental or theoretical construct, the result remains just speculation. In the present case, the MD simulation of the  $\beta$ -lactamase motion in solution certainly suggests that a mechanism of action of the enzyme involving the Glu166 carboxylate as a direct general base catalyst of acylation (**1**) should not be rejected on the basis of the crystal structure alone and may yet represent an element of the true mechanism of class A  $\beta$ -lactamase catalysis.

Reservations concerning the mechanistic conclusions from the MD experiment include, as always, the different time scales involved in the simulation vs that of covalent catalysis (typically microseconds to seconds) and, in this case, some uncertainty as to the state of protonation of the active site functional groups in the active conformation. Further experiment, and possibly also calculation, is needed to clarify the latter point. Probably of more direct relevance to mechanism would be the arrange-

ment in space and the state of protonation of the active site functional groups in the presence of substrates and transition states or their analogues. Such information may well be more directly accessible from theory than experiment. Further research in  $\beta$ -lactamase catalysis will certainly include MD simulations of substrate complexes, acyl-enzymes, and transition state complexes.

**Acknowledgment.** This work was supported through funding from the National Institutes of Health: Grant GM37909 awarded to D.L.B., Grant RR07885-01 awarded to D.L.B. and G.R., and Grant AI17986 awarded to RFP. Grants of computer time and staff support from the Pittsburgh Supercomputing Center and the Frederick Biomedical Supercomputing Center of the Frederick Cancer Research and Development Center are gratefully acknowledged.

JA942197Z